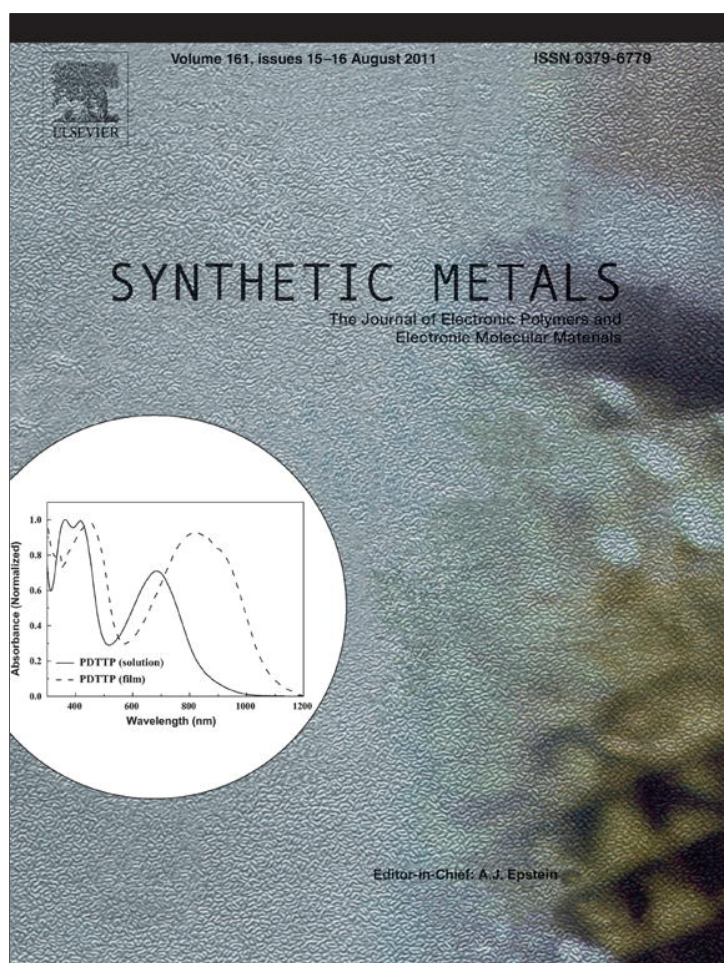


Provided for non-commercial research and education use.  
Not for reproduction, distribution or commercial use.



This article appeared in a journal published by Elsevier. The attached copy is furnished to the author for internal non-commercial research and education use, including for instruction at the authors institution and sharing with colleagues.

Other uses, including reproduction and distribution, or selling or licensing copies, or posting to personal, institutional or third party websites are prohibited.

In most cases authors are permitted to post their version of the article (e.g. in Word or Tex form) to their personal website or institutional repository. Authors requiring further information regarding Elsevier's archiving and manuscript policies are encouraged to visit:

<http://www.elsevier.com/copyright>



Contents lists available at ScienceDirect

## Synthetic Metals

journal homepage: [www.elsevier.com/locate/synmet](http://www.elsevier.com/locate/synmet)

# Synthesis, structure and luminescent properties of 3D lanthanide (La(III), Ce(III)) coordination polymers possessing 1D nanosized cavities based on pyridine-2,6-dicarboxylic acid

Lirong Yang\*, Shuang Song, Caiyun Shao, Wu Zhang, Huaimin Zhang, Zhanwei Bu, Tiegang Ren

Institute of Molecule and Crystal Engineering, College of Chemistry and Chemical Engineering, Henan University, Kaifeng, 475004, PR China

## ARTICLE INFO

## Article history:

Received 11 March 2011

Received in revised form 10 April 2011

Accepted 13 April 2011

Available online 2 July 2011

## Keywords:

Synthesis

Structure

Luminescent properties

Lanthanide coordination polymers

Pyridine-2,6-dicarboxylic acid

## ABSTRACT

Two novel coordination polymers, namely,  $\{[\text{Ln}_2(\text{PDA})(\text{HPDA})(\text{H}_2\text{O})_4\text{ClSO}_4]\cdot 2\text{H}_2\text{O}\}_n$  ( $\text{Ln} = \text{La(III)}$  and  $\text{Ce(III)}$ ) for complexes I and II, respectively) were synthesized through the reaction between pyridine-2,6-dicarboxylic acid ( $\text{H}_2\text{PDA}$ ) and  $\text{La}(\text{NO}_3)_3\cdot 6\text{H}_2\text{O}$  and  $\text{Ce}_2(\text{SO}_4)_3\cdot 8\text{H}_2\text{O}$  under hydrothermal conditions. Both of these polymers possess 1D infinite nanosized cavities embedding guest water molecules. The complexes were characterized by elemental analyses, IR spectroscopy, thermal analyses and single crystal X-ray diffraction. Two compounds crystallize in orthorhombic system, space group  $\text{Pna}2(1)$ . Both of the complexes exhibit 3D metal-organic framework structure, where  $\text{SO}_4^{2-}$  anions play as the bridge between 1D wavelike chains and the adjacent parallel pyridine rings were arranged through  $\pi$ - $\pi$  interactions. The bi-bidentate coordination mode of  $\text{SO}_4^{2-}$  anion was observed. Luminescent emissions of complex I were measured in the solution of DMF at room temperature. In addition, the luminescent emissions of complex I showed certain selectivity among some metal ions.

© 2011 Elsevier B.V. All rights reserved.

## 1. Introduction

The lanthanide-based metal-organic frameworks (Ln-MOFs) have drawn special attention because of their intriguing structure and tremendous potential applications in catalysis, molecular recognitions, optoelectronic devices, sensors, luminescence, molecular magnetism, gas absorption and ion exchange as well as in specifically material sciences [1–6]. A great number of Ln-MOFs have been synthesized and characterized [7–9]. Because their valence orbitals are buried inside [10], lanthanides allow higher coordination number and more flexible coordination geometry than transition metals [11]. It is well known, lanthanide ions have high affinity with hard bases such as oxygen or hybrid oxygen-nitrogen atoms. Consequently, multicarboxylate ligands such as pyridine-2,6-dicarboxylic acid ( $\text{H}_2\text{PDA}$ ) and its deprotonated anions ( $\text{HPDA}^-$  and  $\text{PDA}^{2-}$ ) are in favor of the construction of Ln-MOFs [12–19]. With its rigid  $120^\circ$  angle between pyridine ring and two carboxylate groups, pyridine-2,6-dicarboxylic acid ( $\text{H}_2\text{PDA}$ ) and its deprotonated anions ( $\text{HPDA}^-$  and  $\text{PDA}^{2-}$ ) offers flexible, multidentate coordination sites, and therefore may potentially provide various coordination modes to form discrete or

consecutive metal complexes under appropriate synthesis conditions [20–23].

The present paper is to report the hydrothermal synthesis, characteristics, thermal analysis and the crystal structures of the coordination polymers formed between La(III)/Ce(III) and  $\text{H}_2\text{PDA}$  ligands. The structure of complexes I and II are rather similar, while Ln(III) ions exhibit 10-coordination with the  $\text{N}_2\text{O}_8$  donor set and 8-coordination with the  $\text{O}_7\text{Cl}_1$  donor set. Both of the coordination polymers present 3D architectures with  $\text{SO}_4^{2-}$  anions bridging and  $\pi$ - $\pi$  interactions among adjacent parallel pyridine rings. The striking feature of complexes I and II is that 1D nanosized cavities were observed, where the guest water molecules dwelled. The emission spectra of complex I in the presence of  $\text{Cu}^{2+}$ ,  $\text{Zn}^{2+}$ ,  $\text{Mn}^{2+}$ ,  $\text{Pb}^{2+}$ ,  $\text{Cr}^{3+}$ ,  $\text{Fe}^{2+}$ ,  $\text{Ag}^+$ ,  $\text{Hg}^{2+}$  and  $\text{K}^+$  ions were studied and compared with those of original complex.

## 2. Experimental

## 2.1. Reagents and general techniques

All chemicals are analytical grade and used without further purification.

Elemental analysis was performed on a Perkin-Elmer 240C elemental analyzer. Infrared spectra were recorded in the  $4000\text{--}400\text{ cm}^{-1}$  region using KBr pellets on an AVATAR 360 FT-IR spectrometer, the crystal structure was determined on a Bruker

\* Corresponding author.

E-mail address: [lirongyang@henu.edu.cn](mailto:lirongyang@henu.edu.cn) (L. Yang).

Smart CCD X-ray single-crystal diffractometer. Fluorescent data were collected on F-7000 FL Spectrophotometer at room temperature. The TG and DTG experiment were performed using a Perkin-Elmer TGA7 thermogravimeter. The heating rate was programmed to be 10 K/min with the protecting stream of N<sub>2</sub> flowing at 40 mL/min.

## 2.2. Synthesis of the complexes I and II

### 2.2.1. Synthesis of complex I

Pyridine-2,6-dicarboxylic acid, lanthanum nitrate and cupric sulfate with a molar ratio of 5:2:3 were mixed in 10 mL water and the pH value was adjusted to 3.0 using hydrochloric acid. The mixture was homogenized by stirring for 20 min, and then transferred into 20 mL Teflon-lined stainless steel autoclave under autogenous pressure at 130 °C for 4 days. After cooling the reaction system to room temperature at a rate of 5 °C/h, clear block crystals were isolated. Calc. for I, C<sub>14</sub>H<sub>18</sub>ClLa<sub>2</sub>N<sub>2</sub>O<sub>18</sub>S (%) : C, 19.84; H, 2.14; N, 3.30. Found: C, 19.77; H, 2.09; N, 3.25. IR data (KBr pellet, cm<sup>-1</sup>): 3331 (br), 1612 (s), 1601 (s), 1581 (s), 1468 (s), 1432 (s), 1381 (s), 1273 (s), 1192 (w), 1158 (s), 1071 (m), 1013 (m), 924 (m), 860 (w), 840 (w), 815 (m), 735 (m), 679 (m), 659 (m), 584 (m), 521 (m), 434 (w), 417 (m).

### 2.2.2. Synthesis of complex II

Pyridine-2,6-dicarboxylic acid, cerium sulfate and zinc acetate with molar ratio 5:2:3 were mixed in 10 mL water and the pH value was adjusted to 3.0 using hydrochloric acid. The mixture was homogenized by stirring for 20 min, and then transferred into 20 mL Teflon-lined stainless steel autoclave under autogenous pressure at 130 °C for 4 days. After cooling the reaction system to room temperature at a rate of 5 °C/h, yellow block crystals were isolated. Calc. for II, C<sub>14</sub>H<sub>18</sub>Ce<sub>2</sub>ClN<sub>2</sub>O<sub>18</sub>S (%) : C, 19.78; H, 2.13; N, 3.30. Found: C, 19.56; H, 2.11; N, 3.22. IR data (KBr pellet, cm<sup>-1</sup>): 3422 (br), 1619 (s), 1605 (s), 1560 (s), 1437 (s), 1388 (s), 1365 (m), 1277 (m), 1190 (s), 1159 (m), 1124 (s), 1094 (s), 1012 (m), 929 (m), 862 (w), 846 (w), 771 (m), 729 (m), 654 (m), 607 (m), 523 (w), 434 (m).

## 2.3. X-ray crystallographic determination

Single-crystal X-ray diffraction measurements of complexes I and II were carried out on a Bruker Smart CCD X-ray single-crystal diffractometer. Reflection data were at 293(2) K using graphite monochromated MoK $\alpha$ -radiation ( $\lambda = 0.71073 \text{ \AA}$ ) and the  $\omega$ -scan technique. All independent reflections were collected in a range of 3.26–28.97° for complex I and 2.16–27.54° for II and determined in the subsequent refinement. SADABS Multi-scan empirical absorption corrections were applied to the data processing [24]. The crystal structure was solved by direct methods and Fourier synthesis. Positional and thermal parameters were refined by the full-matrix least-squares method on  $F^2$  using the SHELXTL software package [25]. The final least-square cycle of refinement gave  $R = 0.0278$ ,  $wR = 0.0667$  for complex I and  $R = 0.0590$ ,  $wR = 0.1627$  for II. The crystallographic data, selected bond lengths and bond angles for complexes I and II are listed in Tables 1 and 2, respectively.

## 3. Results and discussion

### 3.1. IR spectra of the complex

Both complexes I and II are stable in air and insoluble in common solvents such as CH<sub>3</sub>COCH<sub>3</sub>, CH<sub>3</sub>CH<sub>2</sub>OH, CH<sub>3</sub>OH, CH<sub>3</sub>CN or THF, but both are soluble in DMF. High yield of the products indicate that the title complexes are thermodynamically stable under the reaction conditions. The IR spectra of two compounds are similar. The broad bands around 3331 and 3422 cm<sup>-1</sup> and peaks at 924 and 929 cm<sup>-1</sup>

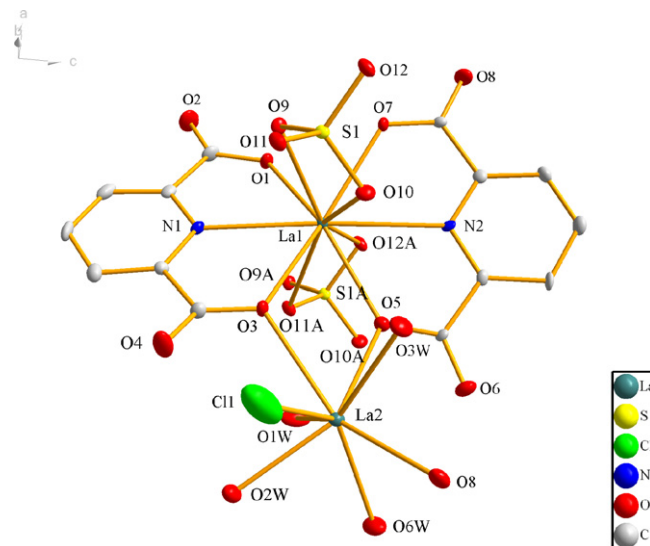
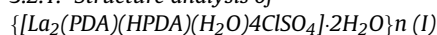


Fig. 1. Coordination environment of complex I with thermal ellipsoids at 30% probability; the asymmetric unit and the related coordination atoms are labeled; lattice water and hydrogen atoms are omitted for clarity.

in complexes I and II are due to water molecules in coordination and lattice forms [26,27]. Each shows strong infrared absorption bands at about 1615 and 1380 cm<sup>-1</sup> that are contributed to the coordinated carboxylates [11]. The IR absorption bands at 1601 and 735 cm<sup>-1</sup> represent the characteristic skeleton vibrations of the pyridine ring. The absorption at 1581 cm<sup>-1</sup> is related to the NH stretching vibration [28]. The absorptions related to the SO<sub>4</sub><sup>2-</sup> ions are also presented in the infrared spectrum. Three bands appearing at 584, 659, and 679 cm<sup>-1</sup> are particularly evident for the  $\nu_4$  mode of SO<sub>4</sub><sup>2-</sup>, and three bands at higher wave numbers (1071, 1158, and 1273 cm<sup>-1</sup>) could be related to  $\nu_3$ . The two bands observed at 1013 and 924 cm<sup>-1</sup> reflect the  $\nu_1$  stretching mode of SO<sub>4</sub><sup>2-</sup>, the one at 924 cm<sup>-1</sup> may be assigned to either  $\nu_1$  or  $\nu_3$  [7,29]. The absorption related to the La–N and La–O stretching vibrations of the complexes were observed at 521–434 cm<sup>-1</sup> [26,27].

## 3.2. Structural description of the complexes

### 3.2.1. Structure analysis of



The molecular structure of complex I is shown in Fig. 1, exhibiting a binuclear lanthanum entity connected by carboxylic oxygen with two types of coordination environments, namely, La1 shows 10-coordination with the N<sub>2</sub>O<sub>8</sub> donor set and La2 shows 8-coordination with the O<sub>7</sub>Cl<sub>1</sub> donor set, respectively. Two kinds of coordination modes *a* and *b* exist in the structure (see Scheme 1). The La1 ion shows a 10-coordinated environment with double-capped cubic prism configuration, two PDA anions act as tridentate (*a* mode) and tetradentate (*b* mode) ligands (ONO) chelated to La1 occupying six coordination sites of the La1 ion, and two sulfate anions act as bidentate ligands (OSO) to fill the remaining four coordination sites. Unchelated PDA ligand on La2 ion was observed. Four molecules of water and three carboxylic oxygen atoms together with one chlorine atom make up the coordination sphere of the La2 center with a geometry of dodecahedron. The La–O bond lengths are from 2.466(5) to 2.685(4) Å, while the bond lengths of La–N are from 2.660(6) to 2.690(6) Å. The bond length observation in the present work is consistent with the previous work for the lanthanide involved polymers [8]. Averagely, La–O<sub>PDA</sub> bonds are longer than La–O<sub>W</sub> bonds. It is noteworthy that La–Cl bond of 2.392(5) Å was formed in the entity of La(III) complex. This is particularly rare in the similar complexes. The bond

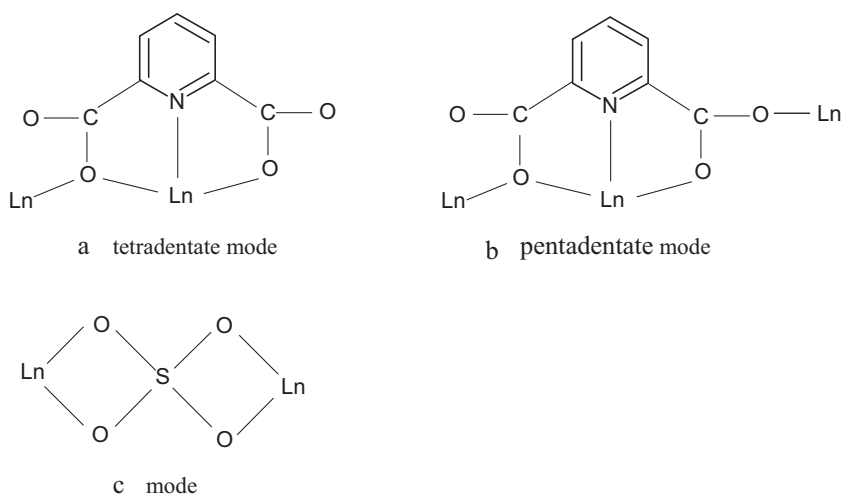
**Table 1**  
Summary of crystallographic data for complexes I and II.

Data	Complex I	Complex II
Empirical formula	C <sub>14</sub> H <sub>18</sub> La <sub>2</sub> ClN <sub>2</sub> O <sub>18</sub> S	C <sub>14</sub> H <sub>18</sub> Ce <sub>2</sub> ClN <sub>2</sub> O <sub>18</sub> S
Formula weight	847.63	850.050
Temperature (K)	293(2)	293(2)
Wavelength (Å)	0.71073	0.71073
Crystal system	Orthorhombic	Orthorhombic
space group	<i>Pna</i> 2(1)	<i>Pna</i> 2(1)
<i>a</i> (Å)	18.8684(4)	18.878(4)
<i>b</i> (Å)	6.57688(13)	6.5818(13)
<i>c</i> (Å)	18.7367(4)	18.732(4)
$\alpha$ (°)	90.00	90.00
$\beta$ (°)	90.00	90.00
$\gamma$ (°)	90.00	90.00
<i>Z</i>	4	4
Density (calculated)	2.421 g cm <sup>-3</sup>	2.416 g cm <sup>-3</sup>
<i>F</i> (000)	1628	1632
Crystal size (mm <sup>3</sup> )	0.22 × 0.20 × 0.18	0.20 × 0.16 × 0.14
$\theta$ range for data collection (°)	3.26–28.97	2.16–27.54
Limiting indices	$-23 \leq h \leq 23, -8 \leq k \leq 8, -23 \leq l \leq 23$	$-24 \leq h \leq 24, -8 \leq k \leq 8, 0 \leq l \leq 23$
Reflections collected/unique	13633/4084 [ <i>R</i> (int)=0.0288]	9194/2758 [ <i>R</i> (int)=0.0530]
Refinement method	Full-matrix least-squares on <i>F</i> <sup>2</sup>	Full-matrix least-squares on <i>F</i> <sup>2</sup>
Data/restraints/parameters	4084/1/379	2758/1/355
Goodness-of-fit on <i>F</i> <sup>2</sup>	1.031	1.013
Volume (Å <sup>3</sup> )	2325.13(8)	2327.4(8)
Final <i>R</i> indices [ <i>I</i> > 2 $\sigma$ ( <i>I</i> )]	<i>R</i> <sub>1</sub> = 0.0278, <i>wR</i> <sub>2</sub> = 0.0667	<i>R</i> <sub>1</sub> = 0.0590, <i>wR</i> <sub>2</sub> = 0.1627
<i>R</i> indices (all data)	<i>R</i> <sub>1</sub> = 0.0270, <i>wR</i> <sub>2</sub> = 0.0660	<i>R</i> <sub>1</sub> = 0.0604, <i>wR</i> <sub>2</sub> = 0.1644
Largest diff. peak and hole/(eÅ <sup>-3</sup> )	0.794 and -1.323	2.334 and -2.149

lengths of La1–S1 and La1–S1A are 3.2855(12) and 3.2923(12) Å, respectively. Considering sum of the van der Waals radii of La and S is slightly longer than 3.4 Å, it is reasonable to assume that there is certain interaction between La and S atoms. Interestingly, there is only one crystallographically independent SO<sub>4</sub><sup>2-</sup> anion in the molecular motif, although two sulfate anions are chelated to a La(III) center. The dihedral angle between pyridine rings connected to the La1 centers is 24.82°, which is a small deviation from the coplanar case. Actually, from the point view of stereochemical effect, the closer the dihedral angle is to 90°, the more stable the configuration of complex I. Obviously, the coordination of SO<sub>4</sub><sup>2-</sup> anions to the La1 ion from both upper and down directions results in such a small dihedral angle. Two sets of oxygen atoms in sulfate anion, (O9, O10) and (O11, O12), and the S1 atom form two planes with a dihedral angle of nearly 90° (88.98°), and the bond lengths of S–O are nearly equal (1.4670(49)–1.4813(42) Å). The angles of O–S–O in a sulfate anion are slightly deviated from those of an ideal tetrahedron, which is sufficient to reduce

the local environmental symmetry from *T<sub>d</sub>* to *C<sub>2v</sub>* for S atom [11].

The coordination polymer consists of the building block of [La<sub>2</sub>(PDA)(HPDA)(H<sub>2</sub>O)<sub>4</sub>ClSO<sub>4</sub>].2H<sub>2</sub>O. La1 and La2 are connected through two carboxylic oxygen (O3, O5) from two PDA<sup>2-</sup> ligands in tridentate *a* and tetradentate *b* modes. The bond lengths are 2.636(4) Å for La1–O3, 2.514(5) Å for La1–O5, 2.685(4) Å for La2–O3 and 2.588(4) Å for La2–O5. Consequently, an approximate rhombus La<sub>2</sub>O<sub>2</sub> grid was formed with the corresponding angles of 62.04(15)° for O5–La1–O3, 60.47(14)° for O5–La2–O3, 114.62(16)° for La1–O3–La2 and 122.80(2)° for La1–O5–La2, respectively. The two La(III) ions are well-separated with the distance of 4.4784(5) Å (La1···La2). The coordination polymer is connected between the adjacent building block of [La<sub>2</sub>(PDA)(HPDA)(H<sub>2</sub>O)<sub>4</sub>ClSO<sub>4</sub>].2H<sub>2</sub>O through carboxylate bridges (OCO). An infinite 1D (La–O<sub>2</sub>–La–OCO–La–O<sub>2</sub>–La)<sub>∞</sub> wavelike chain motif along the *a* axis was formed through the bridges of carboxylate (OCO) and double oxygen alternately. The distances between

**Scheme 1.** Coordination modes of PDA ligand and SO<sub>4</sub><sup>2-</sup> anion.

**Table 2**  
Selected bond lengths (Å) and bond angles (°) for complexes I and II.

<b>Bond lengths</b>					
<b>Complex I</b>					
La(1)–O(1)	2.466(5)	La(1)–S(1A)	3.292(12)	La(2)–O(6W)	2.552(5)
La(1)–O(5)	2.514(5)	La(1)–O(9)	2.664(4)	La(2)–O(8)	2.568(5)
La(1)–O(7)	2.580(4)	La(1)–N(2)	2.690(6)	La(2)–O(5)	2.588(4)
La(1)–O(3)	2.636(4)	La(2)–Cl(1)	2.392(5)	La(2)–O(3)	2.685(4)
La(1)–O(11)	2.639(4)	La(2)–O(1W)	2.498(5)	O(11)–La(1)	2.639(4)
La(1)–O(10)	2.643(4)	La(2)–O(2W)	2.522(5)	O(12)–La(1)	2.724(4)
La(1)–N(1)	2.660(6)	La(2)–O(3W)	2.545(5)	La(1)–O(12)	2.724(4)
La(1)–S(1)	3.286(12)				
<b>Complex II</b>					
Ce(1)–O(1)	2.448(12)	Ce(1)–S(1A)	3.285(3)	Ce(2)–O(16)	2.542(14)
Ce(1)–O(5)	2.511(11)	Ce(1)–O(9)	2.664(11)	Ce(2)–O(8)#2	2.563(14)
Ce(1)–O(7)	2.582(11)	Ce(1)–N(1)	2.676(17)	Ce(2)–O(5)	2.598(10)
Ce(1)–O(4)	2.635(10)	Ce(1)–O(12)#1	2.737(10)	Ce(2)–O(4)	2.683(11)
Ce(1)–O(10)	2.650(11)	Ce(2)–O(15)	2.489(13)	O(8)–Ce(2)#4	2.563(14)
Ce(1)–O(11)#1	2.660(11)	Ce(2)–O(14)	2.526(14)	O(11)–Ce(1)#3	2.660(11)
Ce(1)–N(2)	2.658(18)	Ce(2)–Cl(1)	2.534(14)	O(12)–Ce(1)#3	2.737(10)
Ce(1)–S(1)	3.298(3)				
<b>Bond angles</b>					
<b>Complex I</b>					
O(1)–La(1)–O(5)		152.80(15)		O(1)–La(1)–O(10)	129.09(16)
O(1)–La(1)–O(7)		69.35(15)		O(5)–La(1)–O(10)	78.02(15)
O(5)–La(1)–O(7)		119.67(14)		O(7)–La(1)–O(10)	81.74(14)
O(1)–La(1)–O(3)		121.93(15)		O(3)–La(1)–O(10)	73.92(14)
O(5)–La(1)–O(3)		62.04(15)		O(1)–La(1)–O(9)	78.93(15)
O(7)–La(1)–O(3)		154.73(13)		O(5)–La(1)–O(9)	127.76(15)
O(1)–La(1)–O(11)		82.11(15)		O(7)–La(1)–O(9)	72.16(14)
O(5)–La(1)–O(11)		72.44(15)		O(3)–La(1)–O(9)	87.31(14)
O(7)–La(1)–O(11)		127.91(14)		O(11)–La(1)–O(9)	144.15(15)
O(3)–La(1)–O(11)		77.34(14)		O(1)–La(1)–O(12)	70.29(16)
O(6W)–La(2)–O(5)		106.73(16)		O(5)–La(1)–O(12)	86.27(15)
O(8)–La(2)–O(5)		109.61(16)		O(7)–La(1)–O(12)	77.02(13)
O(1W)–La(2)–O(3)		71.14(17)		O(3)–La(1)–O(12)	127.19(14)
O(2W)–La(2)–O(3)		90.53(14)		O(11)–La(1)–O(12)	52.16(12)
O(3W)–La(2)–O(3)		77.29(16)		O(10)–La(1)–O(12)	142.66(16)
O(6W)–La(2)–O(3)		142.99(17)		O(9)–La(1)–O(12)	142.39(12)
O(8)–La(2)–O(3)		145.09(16)		O(1W)–La(2)–O(5)	67.70(16)
O(5)–La(2)–O(3)		60.47(14)		O(2W)–La(2)–O(5)	133.78(16)
La(1)–O(5)–La(2)		122.80(2)		O(3W)–La(2)–O(5)	67.61(17)
La(1)–O(3)–La(2)		114.62(16)			
<b>Interaction of metal–metal (Å)</b>					
La...La		4.4784(5)		5.2837(5)	6.5769(4)
<b>Complex II</b>					
O(1)–Ce(1)–O(5)		152.5(4)		O(4)–Ce(1)–O(12)#1	127.3(3)
O(5)–Ce(1)–O(7)		120.0(4)		O(11)#1–Ce(1)–O(12)#	152.3(3)
O(5)–Ce(1)–O(4)		62.8(3)		O(15)–Ce(2)–O(14)	69.3(5)
O(1)–Ce(1)–O(10)		129.0(4)		O(14)–Ce(2)–O(17)	143.9(5)
O(7)–Ce(1)–O(10)		81.8(3)		O(14)–Ce(2)–O(16)	73.7(5)
O(1)–Ce(1)–O(11)#1		182.6(4)		O(15)–Ce(2)–O(8)#2	139.9(5)
O(7)–Ce(1)–O(11)#1		128.2(3)		O(17)–Ce(2)–O(8)#2	68.7(4)
O(10)–Ce(1)–O(11)#1		145.6(3)		O(15)–Ce(2)–O(5)	67.6(4)
O(5)–Ce(1)–O(9)		128.6(4)		O(17)–Ce(2)–O(5)	68.4(4)
O(4)–Ce(1)–O(9)		87.6(3)		O(8)#2–Ce(2)–O(5)	109.9(4)
O(11)#1–Ce(1)–O(9)		144.3(4)		O(14)–Ce(2)–O(4)	90.8(4)
O(1)–Ce(1)–O(12)#1		70.3(4)		O(16)–Ce(2)–O(4)	143.4(4)
O(1)–Ce(1)–O(9)		78.5(4)		O(5)–Ce(2)–O(4)	61.0(3)
O(7)–Ce(1)–O(9)		71.4(3)		Ce(1)–O(4)–Ce(2)	114.2(4)
O(10)–Ce(1)–O(9)		52.4(3)		O(1)–Ce(1)–O(7)	115.76(9)
O(5)–Ce(1)–O(12)#1		85.7(4)		O(1)–Ce(1)–O(4)	121.9(4)
O(7)–Ce(1)–O(12)#1		77.2(3)		O(7)–Ce(1)–O(4)	154.7(3)
O(10)–Ce(1)–O(12)#1		142.5(4)		O(5)–Ce(1)–O(10)	78.4(4)
O(9)–Ce(1)–O(12)#1		142.0(3)		O(4)–Ce(1)–O(10)	74.1(3)
O(15)–Ce(2)–O(17)		134.2(4)		O(5)–Ce(1)–O(11)#1	71.9(4)
O(15)–Ce(2)–O(16)		72.1(5)		O(16)–Ce(2)–O(8)#2	70.8(5)
O(17)–Ce(2)–O(16)		133.7(6)		O(14)–Ce(2)–O(5)	134.1(4)
O(14)–Ce(2)–O(8)#2		113.0(4)		O(16)–Ce(2)–O(5)	106.7(4)
O(8)#2–Ce(2)–O(4)		144.9(4)		O(15)–Ce(2)–O(4)	71.4(4)
Ce(1)–O(5)–Ce(2)		121.8(5)		O(17)–Ce(2)–O(4)	76.9(4)
O(4)–Ce(1)–O(11)#1		77.1(3)			
<b>Interaction of metal–metal (Å)</b>					
Ce...Ce		4.4648(10)		5.3004(11)	6.5818(16)

Symmetry transformations used to generate equivalent atoms: #1  $x, y + 1, z$ ; #2  $x - 1/2, -y - 3/2, z$ ; #3  $x, y - 1, z$ ; #4  $x + 1/2, -y - 3/2, z$ .

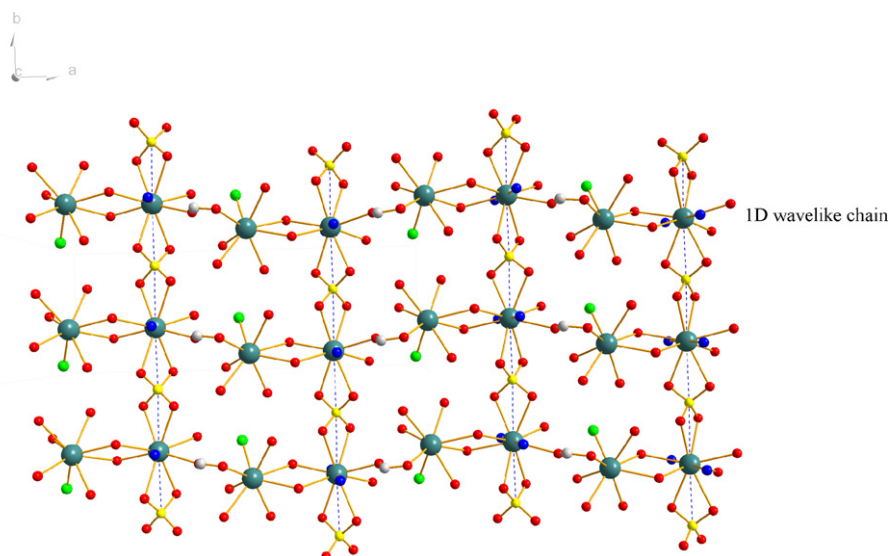


**Fig. 2.** 2D grid motif of complex I constructed by 1D wavelike chains exhibiting the repeat unit structure consisting of  $\text{La}_6\text{C}_2\text{O}_{10}\text{S}_2$  ring and the bi-bidentate coordinated mode of  $\text{SO}_4^{2-}$  anion;  $\text{La} \cdots \text{S}$  weak interaction. Cyan, La; yellow, S; green, Cl; blue, N; red, O; gray, C. (For interpretation of the references to color in this figure legend, the reader is referred to the web version of the article.)

the nonbonding La(III) ions  $\text{La}-\text{O}_2-\text{La}$ ,  $\text{La}-\text{OCO}-\text{La}$  and  $\text{La}-\text{OSO}-\text{La}$  are observed as 4.4784(5), 5.2837(5) and 6.5769(4) Å in the 1-D chain, respectively. Furthermore, the adjacent 1D chains are connected through  $\text{SO}_4^{2-}$  anions from both upper and down directions to construct a highly ordered 2D layer grid along the  $b$  axis [7], as illustrated in Fig. 2. The coordination mode of the sulfate anions in the complex is shown in Scheme 1. The repeat unit in the 2D layer grid exhibits a motif consisting of a hexanuclear homometallic 20-membered  $\text{La}_6\text{C}_2\text{O}_{10}\text{S}_2$  ring with a size of  $10.7251 \text{ \AA} \times 12.4035 \text{ \AA}$  (distances of diagonals). In addition, the parallel pyridine rings of PDA ligands between adjacent 2D layers are partly overlapped (zipper-like) with distances of 3.5588 and 3.5154 Å (centroid to centroid distances between the adjacent pyridine rings). The distance between parallel pyridine rings indicates the strong  $\pi-\pi$  interactions and prepares for the 3D framework with the distance of 9.7521 Å (see Fig. 3) between the adjacent layers. In the framework, 1D nanosized cavities (approximate dimensions of  $6.1805 \text{ \AA} \times 4.4019 \text{ \AA}$ ) present along the  $b$  axis. The La(III) ions, carboxylate oxygen atoms and  $\pi-\pi$  stacking pyridine rings act as walls of the cavities, inside which are occupied by the lattice water molecules. Two water molecules in the lattice are located between two adjacent sheets via hydrogen bonding with one metal bounded water molecule and two carboxylate oxygen atoms (see Fig. 4 and Table 3). Within the infinite 1D nanosized cavities, the embedded guest water molecules are arranged as linear clusters. Each cavity is surrounded by four other identical cavities showing an approximate distance of 9.7640 Å [30,31] (Fig. 5).

### 3.2.2. Structure analysis of

#### $\{[\text{Ce}_2(\text{PDA})(\text{HPDA})(\text{H}_2\text{O})_4\text{ClSO}_4] \cdot 2\text{H}_2\text{O}\}_n$ (II)

The structure of complex II contains the entity  $[\text{Ce}_2(\text{PDA})(\text{HPDA})(\text{H}_2\text{O})_4\text{ClSO}_4] \cdot 2\text{H}_2\text{O}$  in the asymmetric unit as in complex I. Ce1 Exhibits 10-coordination with the  $\text{N}_2\text{O}_8$  donor set with double-capped cubic prism configuration, while Ce2 shows 8-coordination with the  $\text{O}_7\text{Cl}_1$  donor set with dodecahedron geometry. Corresponding figures of II are analogous to those of I.

The bond lengths of Ce–O and Ce–N, as well as the bond angles in the PDA ligands are consistent with the values reported for the similar Ce(III) complexes [32,33,21,34]. The bond lengths

of Ce–Cl is 2.534(14) Å in the entity of Ce(III) complex, much longer than that of La–Cl. The separations of Ce1–S1 and Ce1–S1A are 3.298(3) and 3.285(3) Å, respectively. These are appreciably longer than corresponding bonds in complex I, whereas Ce–N bond lengths are slightly shorter than those in the La–N in complex I. Complex II is assembled by the building block of  $[\text{Ce}_2(\text{PDA})(\text{HPDA})(\text{H}_2\text{O})_4\text{ClSO}_4] \cdot 2\text{H}_2\text{O}$ , which causes an infinite 1D  $(\text{Ce}-\text{O}_2-\text{Ce}-\text{OCO}-\text{Ce}-\text{O}_2-\text{Ce})_\infty$  wavelike chain along the  $a$  axis bridged by carboxylate (OCO) and double oxygen alternately. The nonbonding distances between Ce(III) ions, corresponding to Ce– $\text{O}_2$ –Ce, Ce–OCO–Ce and Ce–OSO–Ce are 4.4648(10), 5.3004(11) and 6.5818(16) Å, respectively.

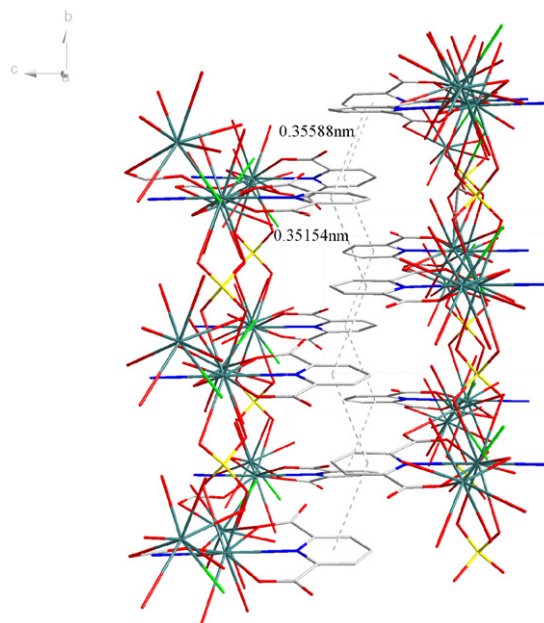


**Fig. 3.** 3D network in complex I constructed by  $\pi-\pi$  stacking interactions. Uncoordinated water and hydrogen atoms were omitted for clarity. Cyan, La; yellow, S; green, Cl; blue, N; red, O; gray, C. (For interpretation of the references to color in this figure legend, the reader is referred to the web version of the article.)

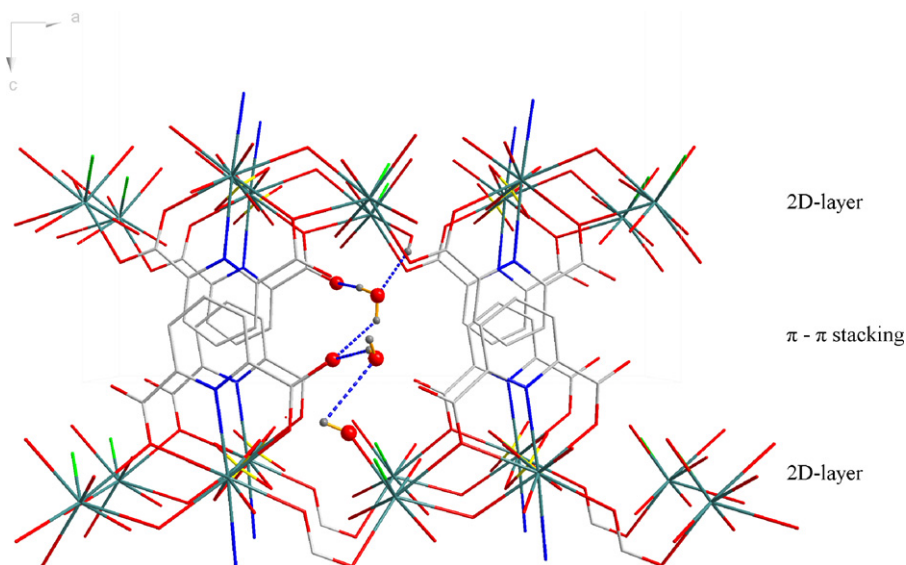


**Fig. 4.** Side view of guest water molecules sandwiched between the  $\pi$ - $\pi$  stacked sheets via hydrogen bonding with the atoms inside the wall in complex I. Cyan, La; yellow, S; green, Cl; blue, N; red, O; gray, C. (For interpretation of the references to color in this figure legend, the reader is referred to the web version of the article.)

The 2D layer grid of complex II exhibits a motif consisting of a hexanuclear homometallic 20-membered  $\text{Ce}_6\text{C}_2\text{O}_{10}\text{S}_2$  ring with a size of  $10.7241 \text{ \AA} \times 12.4061 \text{ \AA}$  (distances of diagonals). The pyridine rings of PDA ligands were orientated parallel with a distance of  $3.5657$  and  $3.5080 \text{ \AA}$  (centroid to centroid distances). A  $\pi$ - $\pi$  interaction established to stabilize the 3D framework, between the neighboring layers is about  $9.7490 \text{ \AA}$ , which is a little shorter than that in complex I. Highly ordered nanosized cavity ( $6.4747 \text{ \AA} \times 4.9317 \text{ \AA}$ ) in complex II is much larger than that in complex I. This is mainly due to lanthanide contraction. The water molecules trapped within the cavity are hydrogen bonded with the oxygen atoms on the walls of the cavity. Each cavity is surrounded by four other identical cavities with an approximate distance of

$9.7585 \text{ \AA}$ . The coordination mode of sulfate anion is similar to that in complex I.

### 3.3. Luminescent properties

As reported in references, the lanthanide ions are useful as luminescent probes and the lanthanide centered emission can be sensitized by molecule of ligands using the  $\pi$  electrons. Significant emission, characteristic of the lanthanide ions may occurred by employing suitable ligands that can absorb and transfer the energy to the central lanthanide ions. Generally, in coordination complexes, the ligand is excited to the singlet state, where part of the energy is transferred to the triplet state through inter system

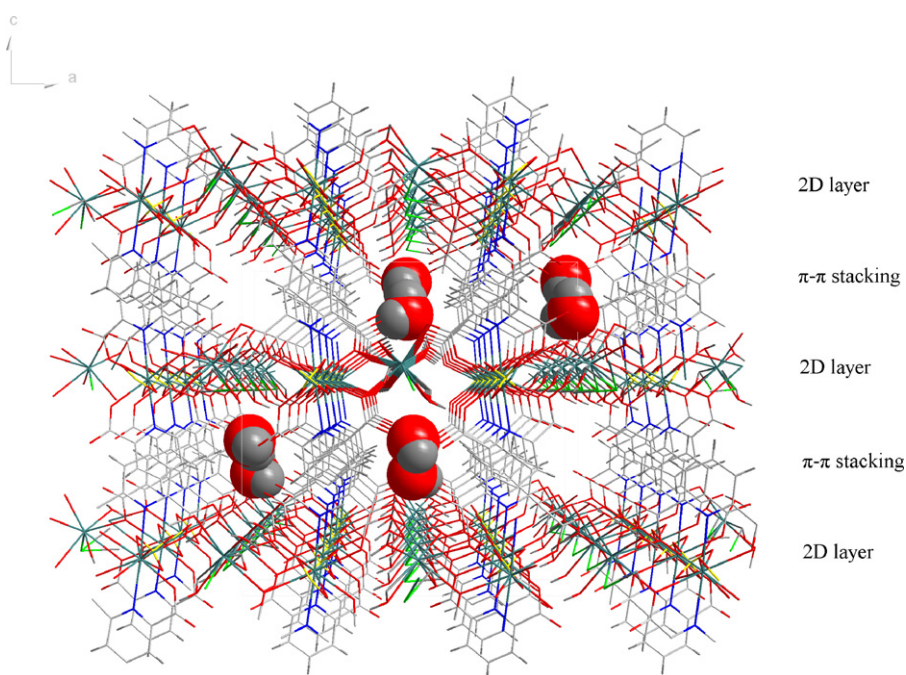


**Fig. 5.** Perspective view of the 3D supramolecular network in complex I, highlighting the infinite 1D parallel cavities with guest water molecules being embedded inside. Cyan, La; yellow, S; green, Cl; blue, N; red, O; gray, C. (For interpretation of the references to color in this figure legend, the reader is referred to the web version of the article.)

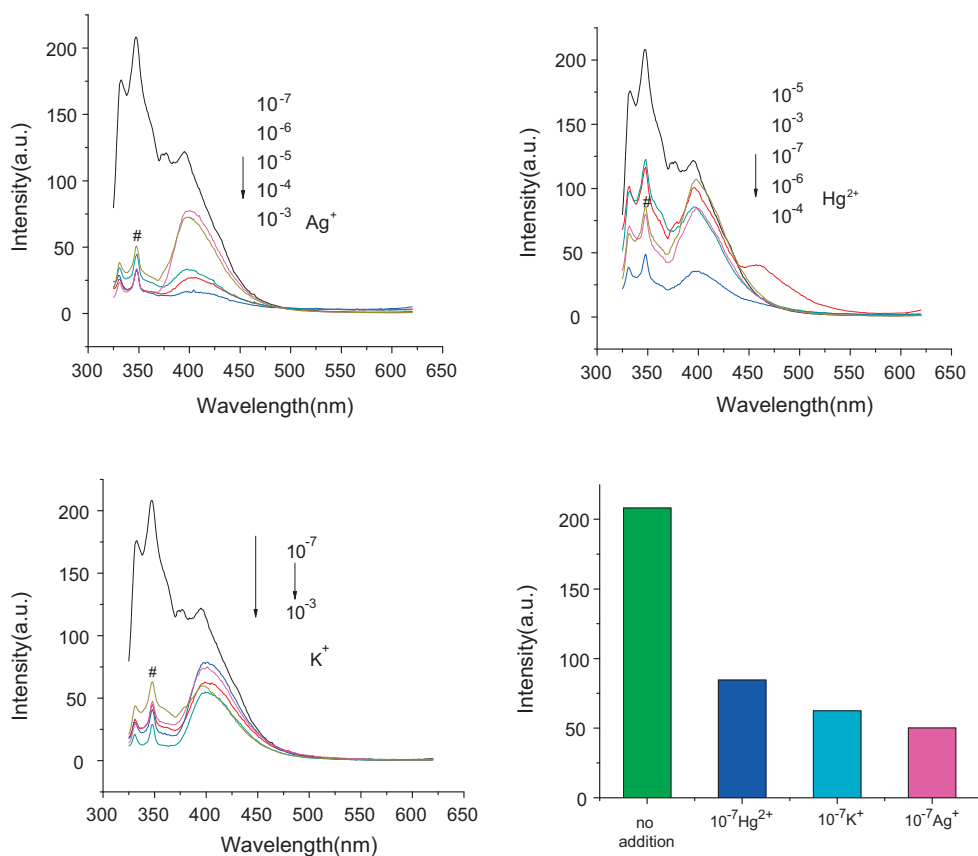


**Fig. 6.** Emission spectra of complex I in DMF ( $10^{-4}$  M) at room temperature in the presence of  $\text{Ag}^+$ ,  $\text{Hg}^{2+}$  and  $\text{K}^+$  ions with respect to complex I (#: ions added with the concentration of  $10^{-7}$  M).

crossing. When the energy levels are favorable, the triplet excited state can transfer the energy to the metal centers, resulting in metal centered luminescence [35–37]. The transfer of energy can be identified by the suppressing of the intra-ligand emission in the luminescence spectra. For the present complexes, the  $\text{PDA}^{2-}$  anions which absorb strongly in the UV region can sensitize the lanthanide ion.

The luminescent properties of complex I were studied in DMF ( $10^{-4}$  M) at room temperature. Emission spectra of I in the presence of  $\text{Ag}^+$ ,  $\text{Hg}^{2+}$  and  $\text{K}^+$  ions with respect to complex I are illustrated in Fig. 6. The emission intensities of complex I decreased significantly upon the addition of  $10^{-7}$ – $10^{-3}$  M of  $\text{Ag}^+$  ( $\text{AgNO}_3$ ),  $\text{Hg}^{2+}$  ( $\text{HgSO}_4$ ) and  $\text{K}^+$  ( $\text{KNO}_3$ ) with respect to I. As the concentration was controlled at

$10^{-7}$  M, the strongest emission at 347 nm for complex I declined to nearly one-third when  $\text{Hg}^{2+}$  was added. It declined to quarter and one-fifth when  $\text{K}^+$  and  $\text{Ag}^+$  were added. As the concentrations of  $\text{Ag}^+$ ,  $\text{Hg}^{2+}$  and  $\text{K}^+$  were adjusted to  $10^{-3}$  M, the luminescent intensities were almost quenched [38]. These results suggest that complex I may be considered as selective luminescent probes of  $\text{Ag}^+$ ,  $\text{Hg}^{2+}$  and  $\text{K}^+$ . Complex I exhibits broad emission bands at 347 and 395 nm (excited at 315 nm), which can be assigned to  $\pi^* \rightarrow n$  or  $\pi \rightarrow \pi^*$  transitions of the coordinated pyridyl rings. Based on the observation above, the emission of complex I may be due to the ligand-to-metal-charge-transfer (LMCT) [39]. Moreover, the luminescent properties of complex I show certain selectivity toward  $\text{Ag}^+$ ,  $\text{Hg}^{2+}$  and  $\text{K}^+$ . In order to make a comparison, the luminescent experiments were performed by adding  $\text{Cu}^{2+}$  ( $\text{Cu}(\text{CH}_3\text{COO})_2$ ),  $\text{Zn}^{2+}$  ( $\text{Zn}(\text{CH}_3\text{COO})_2$ ),  $\text{Mn}^{2+}$  ( $\text{Mn}(\text{CH}_3\text{COO})_2$ ),  $\text{Pb}^{2+}$  ( $\text{Pb}(\text{CH}_3\text{COO})_2$ ),  $\text{Cr}^{3+}$  ( $\text{CrCl}_3$ ), and  $\text{Fe}^{2+}$  ( $\text{FeSO}_4$ ) into the system (Fig. 7). The presence of  $10^{-3}$  M of these transition metals in DMF solutions weakens the luminescent intensity, but the effect was not as strong as that of the  $\text{Ag}^+$ ,  $\text{Hg}^{2+}$  and  $\text{K}^+$  ions. The mechanism of the luminescent feature of the complexes along with its dependence on the co-existing metal ions is still under investigation. Under the same conditions, the luminescent properties of complex II were also measured, the results showed that it has no luminescent selectivity to the metal ions above mentioned.

### 3.4. Thermal analysis

The TG and DTG curves of the complex I in Fig. 8 indicate that the complex decomposes in three steps. The first weight loss stage has a decomposition temperature range of 25–101 °C, with a weight loss of 8.42%. This corresponds to the loss of part of four molecule

**Table 3**  
Hydrogen bonds (Å) and angles (°) for complex I.

D–H...A	d (D–H)	d (H...A)	d (D...A)	(D–H...A)
O1W–H1WA...O6W	0.85	2.39	2.966(8)	125.2
O1W–H1WA...O3W#1	0.85	2.55	3.196(8)	134.2
O2W–H2WA...O9#2	0.85	2.13	2.833(6)	139.6
O2W–H2WB...O6W	0.85	2.30	3.059(7)	149.0
O3W–H3WA...O10	0.85	1.97	2.786(7)	160.0
O3W–H3WB...O4W#3	0.85	2.12	2.791(8)	135.5
O4W–H4WA...O2#4	0.85	2.20	2.830(8)	130.3
O4W–H4WA...O4#5	0.85	2.47	3.195(8)	144.1
O4W–H4WB...O6#6	0.85	2.11	2.879(9)	150.8
O5W–H5WA...O2#7	0.85	2.03	2.770(9)	144.5
O5W–H5WB...O6#8	0.85	2.35	3.088(9)	144.9
O6W–H6WA...O12#2	0.85	2.02	2.834(7)	160.4
O6W–H6WB...O4W#9	0.85	1.97	2.736(8)	149.6

Symmetry transformation used to generate atoms: #1 x, y–1, z; #2 x–1/2, –y+1/2, z; #3 –x+1, –y+1, z–1/2; #4 x–1/2, –y+1/2, z+1; #5 x, y, z+1; #6 –x+1, –y, z+1/2; #7 x, y+1, z+1; #8 –x+3/2, y+1/2, z+1/2; #9 –x+1, –y, z–1/2.

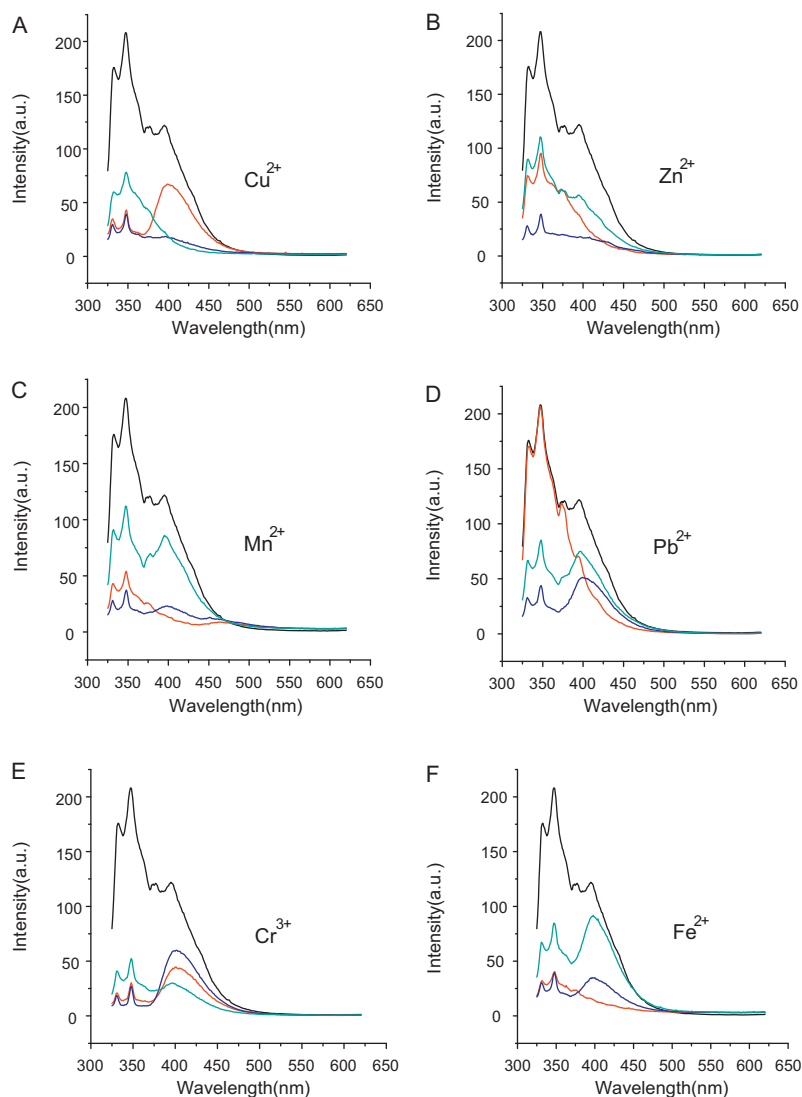


**Fig. 7.** Emission spectra of complex I in DMF ( $10^{-4}$  M) at room temperature (excited at 315 nm) in the presence of  $\text{Cu}^{2+}$ ,  $\text{Zn}^{2+}$ ,  $\text{Mn}^{2+}$ ,  $\text{Pb}^{2+}$ ,  $\text{Cr}^{3+}$  and  $\text{Fe}^{2+}$  ions with respect to complex I, respectively. (A) ( $\text{Cu}^{2+}$ ): black, no addition; blue,  $10^{-4}$  M; green,  $10^{-3}$  M; red,  $10^{-5}$  M. (B) ( $\text{Zn}^{2+}$ ): black, no addition; blue,  $10^{-4}$  M; red,  $10^{-3}$  M; green,  $10^{-5}$  M. (C) ( $\text{Mn}^{2+}$ ): black, no addition; blue,  $10^{-4}$  M; red,  $10^{-3}$  M; green,  $10^{-5}$  M. (D) ( $\text{Pb}^{2+}$ ): black, no addition; blue,  $10^{-4}$  M; red,  $10^{-3}$  M; green,  $10^{-5}$  M. (E) ( $\text{Cr}^{3+}$ ): black, no addition; blue,  $10^{-4}$  M; red,  $10^{-3}$  M; green,  $10^{-5}$  M. (F) ( $\text{Fe}^{2+}$ ): black, no addition; blue,  $10^{-4}$  M; red,  $10^{-3}$  M; green,  $10^{-5}$  M. (For interpretation of the references to color in this figure legend, the reader is referred to the web version of the article.)

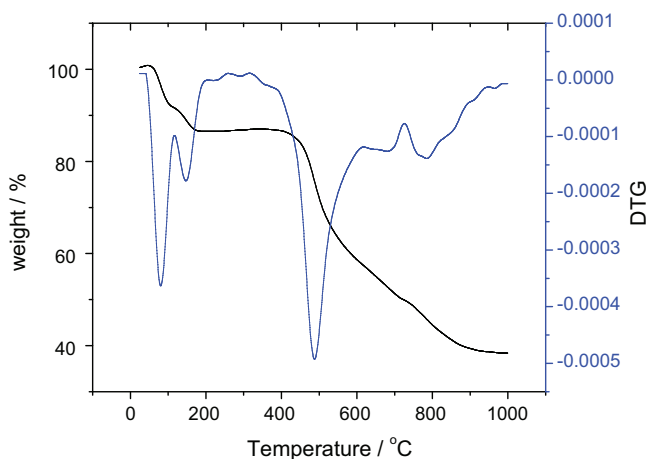


**Fig. 8.** TG and DTG curves of complex I.

of water (theoretical loss is 8.49%). The second weight loss stage has a decomposition temperature range of 101–200 °C, with a weight loss of 6.06%. This can be assigned to the loss of two uncoordinated water molecules (theoretical loss is 6.03%). In the temperature range of 200–400 °C, the complex remains stable. The third weight loss stage has a decomposition temperature range of 400–920 °C, with a weight loss of 47.56%. This is due to the loss of two molecules of  $\text{H}_2\text{PDA}$  ligands, one molecule of sulfate and a chlorine atom (theoretical loss is 47.39%). The final mass remnant of 38.97% is indicative of deposition of  $\text{La}_2\text{O}_3$  (theoretical loss is 38.44%). Complex II undergoes three decomposition steps. The decomposition temperature ranges are similar to those of complex I with the corresponding values of 8.37%, 6.09%, 47.45% and 38.92% (remnant), respectively, which are in accordance with the theoretical values (8.43%, 6.15%, 47.40% and 38.76%).

#### 4. Conclusion

Two similar coordination polymers based on the building block of  $[\text{Ln}_2(\text{PDA})(\text{HPDA})(\text{H}_2\text{O})_4\text{ClSO}_4]\cdot 2\text{H}_2\text{O}$  ( $\text{Ln} = \text{La(III)}$  and  $\text{Ce(III)}$ )

with nanosized cavities were prepared and characterized. Both coordination polymers contain carboxylate bridged infinite 1D  $(Ln-O_2-Ln-OCO-Ln-O_2-Ln)_\infty$  wavelike chain motif. Furthermore, the adjacent 1D chains are connected by  $SO_4^{2-}$  anions to form a highly ordered 2D layer grid through a rarely observed bi-bidentate chelated mode. The repeat unit in the 2D layer grid leads to an entity with a hexanuclear homometallic 20-membered  $Ln_6C_2O_{10}S_2$  ring. In addition, the pyridine rings of PDA ligands between adjacent 2D layers are orientated parallel to generate the 3D framework via  $\pi-\pi$  interactions. In the framework, 1D nanosized cavities are observed to be occupied by the lattice water molecules. Two lattice water molecules are located between the two adjacent 2D layers via hydrogen bonding to one metal-bound water molecule and carboxylate oxygen atoms. Within the infinite 1D nanosized cavities, the embedded guest water molecules are arranged as linear clusters. Finally, the luminescent properties of complex I showed selectivity toward  $Ag^+$ ,  $Hg^{2+}$  and  $K^+$ . Therefore, the complex I may be considered as selective luminescent probe for these metals.

### Supplementary material

CCDC-807630, 807640 contain the supplementary crystallographic data for this paper. These data can be obtained free of charge via [www.ccdc.cam.ac.uk/data\\_request/cif](http://www.ccdc.cam.ac.uk/data_request/cif), or from the Cambridge Crystallographic Data Center, 12 Union Road, Cambridge CB2 1EZ, UK; fax: +44 1223 336 033; or e mail: [deposit@ccdc.cam.ac.uk](mailto:deposit@ccdc.cam.ac.uk).

### Acknowledgments

This work was supported by the Natural Science Foundation of Henan Province, PR China (No. 2010B150005, 092102210172 and 2009B150005).

### References

- [1] M. Eddaoudi, J. Kim, N. Rosi, D. Vodak, J. Wachter, M. O'Keeffe, O.M. Yaghi, *Science* 295 (2002) 469.
- [2] J.S. Seo, D. Whang, H. Lee, S.I. Jun, J. Oh, Y. Jin, Y.J. Jeon, K. Kim, *Nature* 404 (2000) 982.
- [3] F.N. Shi, L. Cunha-Silva, R.A. Sá, L. Ferreira, T. Mafrá, L.D. Trindade, F.A. Carlos, P.J. Almeida, J. Rocha, *J. Am. Chem. Soc.* 130 (2008) 150.
- [4] A.Y. Robin, K.M. Fromm, *Coord. Chem. Rev.* 250 (2006) 2127.
- [5] Y. Ouyang, W. Zhang, N. Xu, G.F. Xu, D.Z. Liao, K. Yoshimura, S.P. Yan, P. Cheng, *Inorg. Chem.* 46 (2007) 8454.
- [6] M. Hu, Q.L. Wang, G.F. Xu, B. Zhao, G.R. Deng, Y.H. Zhang, G.M. Yang, *Inorg. Chem. Commun.* 10 (2007) 1177.
- [7] B. Zhao, L. Yi, Y. Dai, X.Y. Chen, P. Cheng, D.Z. Liao, S.P. Yan, Z.H. Jiang, *Inorg. Chem.* 44 (2005) 911.
- [8] S.K. Ghosh, P.K. Bharadwaj, *Inorg. Chem.* 43 (2004) 2293.
- [9] H.W. Hou, Y.L. Wei, Y.L. Song, Y.T. Fan, Y. Zhu, *Inorg. Chem.* 43 (2004) 1323.
- [10] S.K. Ghosh, P.K. Bharadwaj, *Inorg. Chem.* 44 (2005) 3156.
- [11] N. Tanczecz, C. Feuvrie, I. Ledoux, J. Zyss, L. Toupet, H.L. Bozec, O. Maury, *J. Am. Chem. Soc.* 127 (2005) 13474.
- [12] Y.G. Huang, D.Q. Yuan, Y.Q. Gong, F.L. Jiang, M.C. Hong, *J. Mol. Struct.* 872 (2008) 99.
- [13] T.Y. Zhu, K. Ikarashi, T. Ishigaki, K. ematsu, K. Toda, H. Okawa, M. Sato, *Inorg. Chim. Acta* 362 (2009) 3407.
- [14] B. Zhao, P. Cheng, Y. Dai, C. Cheng, D.Z. Liao, S.P. Yan, Z.H. Jiang, G.L. Wang, *Angew. Chem. Int. Ed.* 42 (2003) 934.
- [15] T.K. Prasad, M.V. Rajasekharan, *Cryst. Growth Des.* 6 (2006) 488.
- [16] B. Zhao, X.Y. Chen, P. Cheng, D.Z. Liao, S.P. Yan, Z.H. Jian, *J. Am. Chem. Soc.* 126 (2004) 15394.
- [17] C.B. Cabarrecq, J.D. Ghys, A. Fernandes, J. Jaud, J.C. Trombem, *Inorg. Chim. Acta* 361 (2008) 2909.
- [18] P. Mahata, K.V. Ramya, S. Natarajan, *Dalton Trans.* 36 (2007) 3973.
- [19] M.O. Rodrigues, N.B. da Costa Junior, C.A. de Simone, A.A.S. Araújo, A.M. Brito-Silva, F.A. Almeida, M.E. de Mesquita, Severino A. Junior, R.O. Freire, *J. Phys. Chem. B* 112 (2008) 4204.
- [20] Y.L. Lu, J.Y. Wu, M.C. Chan, S.M. Huang, C.S. Lin, T.W. Chiu, Y.H. Liu, Y.S. Wen, C.H. Ueng, T.M. Chin, C.H. Hung, K.L. Lu, *Inorg. Chem.* 45 (2006) 2430.
- [21] M.S. Liu, Q.Y. Yu, Y.P. Cai, C.Y. Su, X.M. Lin, X.X. Zhou, J.W. Cai, *Cryst. Growth Des.* 8 (2008) 4083.
- [22] J.P. Leonard, P. Jensen, T. McCabe, J.E. O'Brien, R.D. Peacock, P.E. Kruger, T. Gunnlaugsson, *J. Am. Chem. Soc.* 129 (2007) 10986.
- [23] M.G. Cai, J.D. Chen, M. Taha, *Inorg. Chem. Commun.* 13 (2010) 199.
- [24] G.M. Sheldrick, SADABS: Empirical absorption correction software, University of Göttingen, Institut für Anorganische Chemie der Universität, Tammanstrasse 4, D-3400 Göttingen, Germany, 1999.
- [25] G.M. Sheldrick, SHELXTL: Version 5. Reference manual, Siemens Analytical X-ray Systems, USA, 1996.
- [26] R.R. Tang, G.L. Gu, Q.g. Zhao, *Spectrochim. Acta A* 71 (2008) 371.
- [27] K. Nakamoto, *Infrared and Raman Spectra of Inorganic and Coordination Compounds*, John Wiley and Sons, New York, 1997.
- [28] H. Aghabozorg, A. Moghimi, F. Manteghi, M. Ranjbar, *Z. Anorg. Allg. Chem.* 631 (2005) 909.
- [29] Q.B. Bo, Z.X. Sun, W. Forsling, *Cryst. Eng. Commun.* 10 (2008) 232.
- [30] B. Zhao, P. Cheng, X.Y. Chen, C. Cheng, W. Shi, D.Z. Liao, S.P. Yan, Z.H. Jiang, *J. Am. Chem. Soc.* 126 (2004) 3012.
- [31] X. Feng, X.G. Shi, Q. Sun, L.Y. Wang, J.S. Zhao, Y.Y. Liu, *Synth. React. Inorg. M* 40 (2010) 479.
- [32] C. Brouca-Cabarrecq, J.C. Trombe, *J. Chem. Crystallogr.* 39 (2009) 786.
- [33] C. Brouca-Cabarrecq, J. Dexpert-Ghys, A. Fernandes, J. Jaud, J.C. Trombe, *Inorg. Chim. Acta* 361 (2008) 2909.
- [34] S.K. Ghosh, P.K. Bharadwaj, *Inorg. Chem.* 42 (2003) 8250.
- [35] B.D. Chandler, D.T. Cramb, G.K.H. Shimizu, *J. Am. Chem. Soc.* 128 (2006) 10403.
- [36] P.R. Selvin, *Nat. Struct. Biol.* 7 (2000) 730.
- [37] P. Mahata, K.V. Ramya, S. Natarajan, *Dalton Trans.* 36 (2007) 4017.
- [38] Y.P. Cai, X.X. Zhou, Z.Y. Zhou, S.Z. Zhu, P.K. Thallapally, J. Liu, *Inorg. Chem.* 48 (2009) 6341.
- [39] H. Yin, S.X. Liu, *J. Mol. Struct.* 918 (2009) 165.